

# Accelerator modes of a kicked particle in a square well

R. Sankaranarayanan<sup>1</sup> \*, A. Lakshminarayan<sup>1,2</sup> and V.B. Sheorey<sup>1</sup>

<sup>1</sup>*Physical Research Laboratory, Navrangpura, Ahmedabad 380009, India.*

<sup>2</sup>*Department of Physics, Indian Institute of Technology, Kanpur 208016, India.*

## Abstract

We study accelerator modes of a particle, confined in an one-dimensional infinite square well potential, subjected to a time-periodic pulsed field. Dynamics of such a particle can be described by one generalization of the kicked rotor. In comparison with the kicked rotor, this generalization is shown to have a much larger parametric space for existence of the modes. Using this freedom we provide evidence that accelerator mode assisted anomalous transport is greatly enhanced when low order resonances are exposed at the border of chaos. Quantum dynamical effects of such modes are studied using localized wave packets. Signature of the enhanced transport in the quantum domain is also presented.

## I. INTRODUCTION

In recent years there is a surge of interest in studying mixed systems, with both regular and chaotic regions coexisting in phase space. Mixed systems are important as a majority of dynamical systems found in nature fall in this category. One of the outstanding problems is to resolve how chaotic orbits are influenced by regular regions in the long time limit. In this direction of study, two dimensional area-preserving maps are promising candidates as they exhibit many generic features. A text book paradigm of this kind is the standard map or kicked rotor [1]. One feature of the standard map is that it possesses special kind of orbits called *Accelerator Modes* (AM) [2]. If an initial state of the rotor corresponds to the AM, then it is uniformly accelerated after each kick. In other words, momentum of the rotor increases linearly with time. This is to be contrasted with generic chaotic orbits that diffuse in momentum, i.e., momentum variance of an ensemble of chaotic orbits increases linearly in time leading to *normal diffusion*.

AM are seen in phase space as small regular islands embedded in a chaotic sea. They are separated from chaotic region by cantori (partial-barriers). If a chaotic orbit enters through the cantori, it sticks to the cantori for very long time and thus is accelerated along with the modes. Considering  $n$  as time, such a long excursion of a chaotic orbit is an example of *Lévy flight* [3]. Levy flight, some times called as *super diffusion*, is characterized by  $\langle p_n^2 \rangle \sim n^\gamma$

---

\*Present Address: Department of Physics of Complex Systems, Weizmann Institute of Science, 76100 Rehovot, Israel.

with  $\gamma > 1$ . AM assisted anomalous transport of this kind has been already studied with different motivations [4]. It should be noted that the above mechanism of anomalous effect is numerically ascertained. We demonstrate that when the border of AM (which we call a “beach”) is such that it exposes a large chain of islands of a small order resonance the “stickiness” of the AM increases significantly leading to enhanced anomalous transport.

In chaotic quantum systems it is important to know the dynamics and effects of these modes. An earlier study on the quantized kicked rotor shows that survival probability of a wave function in AM decays exponentially with time and the decay rate is  $\beta \sim \exp(-1/\hbar)$  [5]. Loss of probability, interpreted as barrier-penetration, reduces the effect of modes upon quantization. Recently, such decay has been understood to an extent using a simple model [6]. Developments on confining atoms in magneto-optical traps have opened experimental feasibility for atom-optics realizations of the kicked rotor. One such realization, in which an ensemble of cold cesium atoms are exposed to a periodically pulsed standing wave light, has shown that for certain values of the kick amplitude the momentum distribution of the atomic sample is non-exponentially localized [7]. This then is shown as an effect of AM in the quantum system. A similar experiment, wherein sample of atoms are allowed to interact with pulsed standing wave in presence of gravity, demonstrated a pure quantum mechanical technique for imparting large amount of momentum to the cold atoms [8]. This technique, termed as *quantum accelerator modes*, is supported by a subsequent theoretical work [9].

Semiconductor based technological developments, on the other hand, have shown that it is possible to fabricate potential wells on atomic scales. Motion of electrons in such quantum wells in presence of an external electromagnetic field has been studied for experimental signatures of quantum chaos [10]. A simple model of this kind is a particle confined in a one-dimensional infinite square well exposed to a time periodic pulse field. This system is known to be one generalization of the kicked rotor [11]. The virtue of this generalization arises from two length scales of the system, namely, the well width and the field wavelength. If the well width is an integer multiple of the field wavelength, kick to kick dynamics of the particle is equivalent to that of the rotor. Otherwise, the dynamics is described by a discontinuous map resulting in a new scenario for transition to chaos even for weak field strengths [11].

In this paper we explore this model in the context of their AM. We show that, our generalization leads to a larger parametric space, in comparison to the standard map, for existence of the AM. For certain values of the additional parameters the AM are surrounded by beach regions, that are intermediate sticky regions sandwiched between a large regular chain of islands and the chaotic sea. Beaches are known to significantly influence dynamical tunnelling in quantum systems [12]. We provide evidence to show that beaches are mainly responsible for the AM assisted anomalous transport. In later part of the paper, we investigate in detail the influence of AM in the quantum regime using localized wave packet. This is in contrast to the earlier works on kicked rotor where the momentum eigenstate was used as an initial state.

## II. CLASSICAL SYSTEM

### A. The Map

Let us consider a particle confined in an one-dimensional infinite square well potential  $V_0(x)$  of width  $2a$  and the Hamiltonian is

$$H_0 = \frac{p^2}{2M} + V_0(x) \quad ; \quad V_0(x) = \begin{cases} 0, & \text{for } |x| < a \\ \infty, & \text{for } |x| \geq a \end{cases} . \quad (1)$$

The particle is subjected to a time periodic pulsed field of period  $T$ . The perturbed system is governed by the Hamiltonian

$$H = H_0 + \epsilon \cos\left(\frac{2\pi x}{\lambda}\right) \sum_n \delta\left(n - \frac{t}{T}\right) \quad (2)$$

where  $\epsilon$  and  $\lambda$  are strength and wavelength of the field respectively; a train of delta functions accomplishes the time periodic pulse. Kick to kick dynamics of the particle can be described by the map

$$\begin{aligned} X_{n+1} &= (-1)^{B_n} (X_n + P_n) + (-1)^{B_n+1} \text{Sgn}(P_n) B_n \\ P_{n+1} &= (-1)^{B_n} P_n + (K/2\pi) \sin(2\pi R X_{n+1}) \end{aligned} \quad (3)$$

where  $B_n = [\text{Sgn}(P_n)(X_n + P_n) + 1/2]$ ;  $[..]$  and  $\text{Sgn}(..)$  stand for integer part and sign of the argument respectively.  $B_n$  is the number of bounces of the particle between the walls during the interval between  $n$ th and  $(n+1)$ th kick. This dimensionless map is related to physical variables by the scaling:

$$X_n = \frac{x_n}{2a}, \quad P_n = \frac{p_n T}{2aM}, \quad K = \frac{2\epsilon\pi^2 T^2}{aM\lambda}, \quad R = \frac{2a}{\lambda} \quad (4)$$

where  $K$  is effective field strength and  $R$  is ratio of two length scales of the system. Henceforth we refer to the classical mapping (3) as the *well map*.

The well map can be studied by invoking a *Generalized Standard Map* (GSM)

$$\begin{aligned} J_{n+1} &= J_n + (K/2\pi) \sin(2\pi R \theta_n) \\ \theta_{n+1} &= \theta_n + J_{n+1} \quad (\text{mod } 1) \end{aligned} \quad (5)$$

since time reversal of GSM and (3) are quantitatively related. GSM is defined on a cylinder  $(-\infty, \infty) \times [-1/2, 1/2]$  and the standard map is a special case with  $R = 1$ . A detailed study of GSM can be found in our earlier work [11]. The GSM is highly chaotic for strong field strength (large  $K$ ). In addition, it exhibits chaotic motion even for weak field strength (small  $K$ ) depending on the parameter  $R$ . In order to study the AM in the well map, we invoke the GSM which is amenable to a detailed analysis.

## B. Stability Analysis

Periodicity of the GSM in  $J$  and  $\theta$  (with unit period) implies existence of AM. These are located at  $(J', \theta')$ :

$$J' = m \quad ; \quad \frac{K}{2\pi} \sin(2\pi R\theta') = l \quad (6)$$

where  $m$  and  $l$  are integers. They are also termed as step- $|l|$  AM as the acceleration is  $|l|$  at each iteration. Fixed points belong to the family of AM with  $l = 0$ . For stable AM, required stability condition is

$$-\frac{4}{KR} < \cos(2\pi R\theta') < 0 \quad (7)$$

and using (6) this becomes

$$|l| < \frac{K}{2\pi} < \sqrt{l^2 + \left(\frac{2}{\pi R}\right)^2}. \quad (8)$$

This inequality can also be rewritten as

$$0 < R < R_1 \quad (9)$$

where  $R_1 = (2/\pi) \left\{ (K/2\pi)^2 - l^2 \right\}^{-1/2}$ .

For stable AM

$$|\theta'| = \frac{1}{2R} \left\{ 2j + 1 \mp \frac{1}{\pi} \sin^{-1} \left( \frac{2\pi|l|}{K} \right) \right\} \quad (10)$$

where  $j$  is an integer. Thus the AM are characterized by two integers  $l$  and  $j$  and we call them as  $(l, j)_+$  type modes. Since the cylindrical phase space of GSM has the constraint  $|\theta'| \leq 1/2$  (equivalent to restriction of the particle dynamics to between walls of the well), zero can not be lower limit in the above inequality.

The parameter  $R$  in GSM is recognized as frequency of the sinusoidal force term. As  $R$  increases from zero  $|\theta'|$  decreases such that  $(l, j)_-$  type modes first appear in the phase space followed by the  $(l, j)_+$  type. In a similar way, as  $R$  decreases  $|\theta'|$  increases such that  $(l, j)_+$  type is the first to disappear from the phase space while the  $(l, j)_-$  type mode is the last to disappear. Hence, lowest limit for the inequality (9) is set by the disappearance of  $(l, j)_-$  type modes. From Eqn. (10), the constraint  $|\theta'| \leq 1/2$  for  $(l, j)_-$  becomes  $R_0 \leq R$  where  $R_0 = 2j + 1 - (1/\pi) \sin^{-1}(2\pi|l|/K)$ . Thus the inequality (9) is replaced by

$$R_0 \leq R < R_1. \quad (11)$$

We emphasize that both the inequalities (8) and (11) must be simultaneously satisfied for existence of AM in the phase space. This is in contrast to the standard map for which the inequality (8) with  $R = 1$  itself is sufficient. Thus the two control parameters,  $K$  and  $R$ , provide a larger parametric space, in comparison to that of the standard map, for the existence of AM. At  $K = 2\pi|l|$ , the lower bound of the inequality (8),  $R_0 = 1/2$  and this is the minimum possible value of  $R_0$ . In other words, for  $R < 1/2$  AM do not exist. In fact, GSM is hyperbolic for  $R < 1/2$  and there are only unstable orbits in the phase space.

### C. Results

Since the well map and the GSM are quantitatively related, location of AM are same for both the maps i.e.,  $(X', P') = (\theta', J')$  and all the above arguments hold for well map also. However, AM of the well map differ only in the following way due to the reflective boundary condition. When particle is on the AM,  $n$ th kick causes the particle to undergo  $n$  bounces between the walls. If  $n$  is odd momentum changes its sign, in turn sign of the particle position is also flipped.

Phase space of a mixed system generally has an intricate structure. In particular, boundaries of regular structures embedded in chaotic region have structures at all scales and all of them are hard to discern. Stable AM slands are believed to be separated from the remaining chaotic region by cantori (partial-barriers). Phase space in the vicinity of the cantori is sticky as it retains long time correlations. When chaotic orbits explore all parts of the phase space, there are occasions that they pass through the cantori. When such an event occurs, chaotic orbits stick to the vicinity of cantori for long time. Thus they are dragged along the modes ballistically [13]. This is a mechanism which is known to enhance momentum transport. Below we demonstrate that the beaches around the AM island when occupied by a large resonance of small order are much more sticky. This in turn implies that the cantori surrounding these must have large gaps to allow larger penetration of itinerant chaotic orbits.

Before we dwell more on AM assisted super diffusion, it is instructive to look at some of the modes of the well map. Fig. 1 shows islands for different  $R$  values. In the given range of phase space we find one  $(1, 0)_-$  type mode for  $R = 0.7, 0.8$  and  $1$ . As  $R$  increases the islands move towards interior of the well. For  $R = 1.4$ , one more mode just appears at boundary of the well. This is a  $(1, 0)_+$  type mode. For further large values of  $R$  both the types fully appear and they move into the interior of the well. Evidently, parameter  $R$  also changes the size of the islands.

In order to quantify the role of  $R$  in AM assisted anomalous transport, we consider  $\langle (P_n - P_0)^2 \rangle \sim n^\gamma$ . Here the angular bracket stands for an ensemble average and the exponent can be evaluated by iterating an ensemble of phase space points for long time under the well map. We perform numerical calculations for two different initial ensembles: (i) phase space points uniformly distributed along the line  $P_0 = 0$  which correspond to *both* accelerator and chaotic orbits; (ii) phase space points from a chaotic region which include *only* chaotic orbits.

The ensemble (i) contains more chaotic orbits than the regular (accelerator) orbits. Chaotic orbits exhibit normal diffusion in momentum i.e., like the random walk, until they are dragged along the mode. On the other hand, the accelerator orbits exhibit ballistic behaviour ( $\gamma = 2$ ). Hence, in the long time limit, evolution of accelerator orbits dominate the ensemble average. Fig. 2(i), shows the characteristic exponent  $\gamma$  for different  $R$  values. As we see, for the range of  $R$  in Eqn. (11)  $\gamma \simeq 2$ , confirming the existence of AM islands. Here the lesser  $\gamma$  for  $R = 1.5$  is attributed to small size of AM (see Fig. 1). On contrary, for parameters outside the range of Eqn. (11), diffusion is normal as there are no AM in the phase space.

Fig. 2(ii) corresponds to the ensemble which contains only chaotic orbits. Within the parametric range where AM exist, the exponent  $\gamma$  shows large fluctuations. There are

also occasions wherein presence of AM does not enhance the diffusion significantly. It is natural to attribute the observed fluctuations to size of the islands and stickiness of their neighbourhood. That is, big AM islands with very sticky neighbourhood can significantly enhance the transport.

For  $R = 0.8$ , the exponent  $\gamma$  is found to be maximum ( $\simeq 1.6$ ). As seen from Fig. 1, in this case AM island is surrounded by a chain of 1/5 resonance zones. These zones are also step-1 accelerators and they are separated from chaotic region by their boundary, the so called “beaches”. Dynamics on the beach is chaotic, but very sticky with longer classical staying time. If a wandering chaotic orbit happens to approach the beach region, it stays there for long time and thus gets accelerated along the modes resulting in very large enhancement in momentum transport. This maximum transport is a generic behaviour i.e., independent of choice of the chaotic ensemble. We shall note from Fig. 1 that, although size of the AM for  $R = 0.7$  is larger than that for  $R = 0.8$ , exponent  $\gamma$  is maximum for the later. This shows that beaches accompanying the modes are *mainly* responsible for AM assisted anomalous transport. Thus the well map or equivalently GSM has a control parameter  $R$  by tuning which AM induced super diffusion can be maximized.

Moreover, longer the period of resonance zones lesser the stickiness of associated beach regions. Upon magnifying boundaries of AM islands for  $R = 0.7$  and 1, we found long chain of resonance zones and their beach regions. As seen from Fig. 2, enhancement is limited for both these cases.

Further, we explore step-2 AM which are smaller in size than the step-1 modes. We choose  $K/2\pi = 2.05$  and step-2 modes exist in the range  $0.57 < R < 1.41$ . Nearly ballistic evolution in this range and the otherwise normal diffusion are shown in Fig. 3(i). In Fig. 3(ii) the exponent exhibits large fluctuations. In order to appreciate the role of beach regions in large scale transport, we focus our attention on two distinct cases where the exponent shows a minimum and a maximum. As we see from Fig. 4, when the enhancement is minimum (or absent) AM islands do not have the surrounding beach regions. On the other hand, when AM island is escorted by short chain of resonance zones and their beach regions transport is maximum. These results reinforce that sticky beach regions around AM island are the principal candidates for momentum enhancement.

### III. QUANTUM SYSTEM

#### A. The Map

In a similar manner to that for the classical system, the kick to kick quantum dynamics can be studied using quantum map by solving Schrödinger equation for one period  $T$  as

$$|\psi(t+T)\rangle = U|\psi(t)\rangle \quad (12)$$

where  $U = \exp\{-ik \cos(2\pi x/\lambda)\} \exp\{-iH_0 T/\hbar\}$  with  $k = \epsilon T/\hbar$ , being the effective field strength. Eigenvalue equation of the unperturbed system is  $H_0|\phi_n\rangle = E_n|\phi_n\rangle$ . The eigenstates and eigenvalues are given by

$$\langle X|\phi_n\rangle = \begin{cases} \sqrt{2} \cos(n\pi X), & \text{for } n \text{ odd} \\ \sqrt{2} \sin(n\pi X), & \text{for } n \text{ even} \end{cases} ; \quad E_n = \frac{n^2\pi^2\hbar^2}{2M} \quad (13)$$

with  $n = 1, 2, 3 \dots$ . Considering unperturbed eigenstates as the basis, time evolution of an arbitrary quantum state is  $|\psi(t)\rangle = \sum_n A_n(t)|\phi_n\rangle$  where  $A_n(t) = \langle\phi_n|\psi(t)\rangle$ . With following substitution

$$\tau = \frac{E_n T}{\hbar n^2} = \frac{\pi^2 \hbar T}{2M} \quad (14)$$

quantum map (12) takes the form

$$A_m(t+T) = \sum_n U_{mn} A_n(t) \quad (15)$$

where  $U_{mn} = e^{-i\tau n^2} \langle\phi_m| \exp\{-ik \cos(2\pi RX)\} |\phi_n\rangle$ .

Dimensionless quantum parameters  $k, \tau$  and the classical parameters are related through  $K/R = 8k\tau$ . Since  $k \sim 1/\hbar$  and  $\tau \sim \hbar$ , semiclassical limit for given classical system can be achieved by taking the limits  $k \rightarrow \infty$  and  $\tau \rightarrow 0$ . In the following numerical calculations, quantum map (15) is implemented with a finite, say  $N$ , number of unperturbed basis states. By obtaining the limit

$$\lim_{N \rightarrow \infty} \sum_{n=1}^N |A_n(t)|^2 \rightarrow 1 \quad (16)$$

we ensure that such a truncation of basis does not influence the quantum system.

As seen from Eqn. (15), unperturbed motion of the particle between successive kicks just adds phase to the wave function components through the parameter  $\tau \pmod{2\pi}$ . If  $\tau = 2\pi$ , unperturbed motion is absent and this is called *quantum resonance*. Under this condition, without loss of generality, we can write

$$|\psi(t)\rangle = e^{-ik \cos(2\pi RX)t} |\psi(0)\rangle \quad (17)$$

where  $t$  represents the number of kicks. Then in the limit  $t \rightarrow \infty$ , kinetic energy of the particle grows quadratically i.e.,  $\langle E \rangle_t \sim t^2$  [14]. This phenomenon is similar to that of the quantum kicked rotor [15]. An earlier study has shown that quantum resonance of kicked rotor occurs when  $\tau$  is rational multiples of  $2\pi$  [16]. This non-generic pure quantum phenomenon does not have any classical analogue. In order to investigate signatures of AM in the quantum system, it is necessary to suppress the resonance effect. This can be accomplished by taking  $\tau$  as an irrational multiple of  $2\pi$ .

## B. Initial wave packet

The simulation of AM and their effects in quantum regime is investigated by considering the evolution of an initially localized wave packet. We take a Gaussian wave packet confined in the square well as the initial state. In position representation it is given by

$$\langle X|\psi(0)\rangle = C \exp \left\{ -\frac{(X - \langle X \rangle)^2}{2\sigma^2} + \frac{i\langle P \rangle X}{\hbar_e} \right\} \quad (18)$$

where  $\sigma$  measures width of the wave packet, centred at  $\langle X \rangle$  with momentum  $\langle P \rangle$ . Here  $\hbar_e = 2\tau/\pi^2$  is the effective Planck constant. Normalization constant,  $C$ , is obtained from the condition

$$\int_{-1/2}^{1/2} |\langle X | \psi(0) \rangle|^2 dX = 1$$

as

$$C = \left( \frac{2/\sigma\sqrt{\pi}}{\operatorname{erf}(y_+) - \operatorname{erf}(y_-)} \right)^{\frac{1}{2}} \text{ with } y_{\pm} = \frac{\pm 1/2 - \langle X \rangle}{\sigma}. \quad (19)$$

As the quantum map is described in unperturbed basis states, the initial wave packet is represented in this basis. For evaluating  $A_n(0)$  we consider following integral

$$G_n = \sqrt{2} \int_{-1/2}^{1/2} e^{in\pi X} \langle X | \psi(0) \rangle dX. \quad (20)$$

With change of variable  $u = (X - \langle X \rangle)/\sqrt{2}\sigma$  the integral becomes

$$G_n = 2\sigma C e^{iz_n \langle X \rangle} \int_{u_-}^{u_+} e^{-(u^2 - i\sqrt{2}\sigma z_n u)} du \quad (21)$$

where  $z_n = n\pi + \langle P \rangle/\hbar_e$  and  $u_{\pm} = y_{\pm}/\sqrt{2}$ . Using the standard integral [17]

$$\int e^{-(a_o x^2 + 2bx + c)} dx = \frac{1}{2} \sqrt{\frac{\pi}{a_o}} \exp\left(\frac{b^2 - ca_o}{a_o}\right) \operatorname{erf}\left(\frac{a_o x + b}{\sqrt{a_o}}\right) \quad (22)$$

$G_n$  is represented in terms of complex error function, which can be computed using the algorithm [18]. The wave packet in the unperturbed basis is then given by

$$A_n(0) = \begin{cases} (G_n + G_{-n})/2, & \text{for } n \text{ odd} \\ (G_n - G_{-n})/2i, & \text{for } n \text{ even} \end{cases}. \quad (23)$$

It should be noted that because of the spatial confinement, the initial state is a truncated Gaussian and hence it is *not* a minimum uncertainty wave packet. However, it can be made close to the minimum uncertainty wave packet provided mean  $\langle X \rangle$  is not close to boundary of the well and  $\Delta X \ll 1$ , i.e., spread in position is much less than the width of the square well. With this condition on the wave packet we consider the uncertainty relation  $\Delta X \Delta P = \hbar_e/2$  for the following exercise. We take  $\Delta X = 0.02$  throughout.

## C. Results

To simulate quantum evolution of the AM, the classical system with parameter values  $K/2\pi = 1.05$ ,  $R = 0.9$  is considered. The corresponding phase space with AM island is shown in Fig. 5. In order for generic case of the quantum system, i.e., excluding quantum resonance, we take  $\tau = 2\pi gh'$  where  $g = (\sqrt{5} - 1)/2$  is the most irrational number (golden mean) and  $h'$  is the scaled Planck constant ( $h' = 1.27\hbar_e$ ).

Initial wave packets are chosen such that influence of AM can be contrasted from chaotic motion. Quantum evolution is performed for two initial wave packets: (a) one is placed *on* the AM with  $(\langle X \rangle, \langle P \rangle) = (X', P') = (0.33, 0)$  and (b) the other is placed *outside* the AM with  $(\langle X \rangle, \langle P \rangle) = (0, 0.5)$ . Dimensionless kinetic energy of the time evolved state is given by

$$\langle E \rangle_t = \langle \psi(t) | \hat{P}^2 | \psi(t) \rangle = \left( \frac{2\tau}{\pi} \right)^2 \sum_{n=1}^N |A_n(t)|^2 n^2 \quad (24)$$

which is equivalent to the classical energy  $\langle P_t^2 \rangle$ . Here the number of basis states considered is as high as  $N = 7500$ .

At first, we proceed for the case (a) in the limit  $h' \rightarrow 0$ . In this semiclassical limit the effective field strength  $k$  becomes large, causing rapid spread of the wave packet in the unperturbed basis states. This demands practically infinite number of basis states to uncover long time behaviour. With this numerical limitation in mind, we focus attention on short time evolution. Since  $\Delta X$  is fixed, for large  $h'$  initial wave packet has more spread in momentum. In other words, the wave packet contains both regular and chaotic components. As  $h'$  reduces, initial wave packet contains more regular components of the AM and less chaotic components.

Considering power law behaviour for the quantum energy as  $\langle E \rangle_t \sim t^\gamma$ , Fig. 6 shows the exponent  $\gamma$  as a function of scaled Planck constant. As  $h'$  decreases from 0.01 to 0.001,  $\Delta P$  decreases from 0.2 to 0.02. In the limit  $h' \rightarrow 0$ , the exponent increases and this is due to more accelerator (regular) components in the wave packet. For  $h' = 0.001$  or  $\Delta P = 0.02$  ( $= \Delta X$ ), the initial wave packet is circular in  $X - P$  space and it has only regular components. This is evident as the wave packet is confined within the stable region of AM (see Fig. 5). Here the energy of the evolved wave function grows quadratically in time ( $\gamma \approx 2$ ).

For comparison we have also shown classical exponent in Fig. 6. Classical exponent is evaluated from an ensemble of initial points which are Gaussian distributed with same mean and variance as that of the initial state. Deviation between quantum and classical exponent decreases with  $h'$ . In other words, quantum-classical deviation is proportional to the fraction of chaotic components of the initial state. If the wave packet has any chaotic components it loses its shape very rapidly and fails to show the underlying classical behaviour. For  $h' = 0.001$ , as chaotic components are absent, quantum evolution agrees with the classical evolution.

In Fig. 7 time evolution of energy is shown for the cases (a) and (b) with  $h' = 0.001$ . While the energy grows quadratically in time for the former, it grows linearly in time for the later. Corresponding wave packet dynamics are shown in Fig. 8. We may recollect that classical dynamics of AM for the well system is such that both position and momentum flip their sign for odd number of kicks. In Fig. 8(a), the evolved wave packet reproduces underlying classical behaviour of AM. Thus we have simulated quantum dynamics of AM using localized wave packet with good quantum-classical correspondence. On contrary, wave packet in Fig. 8(b) loses its shape and spreads all over the square well very rapidly. This is indeed a typical behaviour of a wave packet localized initially in chaotic regions of phase space. In such an evolution, quantum interference governs long time dynamics.

Finally, it is natural to look for quantum manifestation of the beaches if any. For that we consider case (b) and perform long time quantum evolution. The results are shown in Fig.

9. In all the cases, initially the quantum energy increases and then attains a quasiperiodic saturation. However, the saturation is much higher for  $R = 0.8$  than for  $R = 0.7$  and 1. It should be noted that even though effective field strength  $k$  is larger for  $R = 0.7$  than for  $R = 0.8$ , energy saturation for the later is much higher. We may compare these results with the corresponding phase space shown in Fig. 1. Thus we obtain a clear evidence that though beaches around AM island are classical structures their presence is felt in quantum dynamics.

#### IV. CONCLUSION

We studied accelerator modes for a particle inside a 1D infinite square well in presence of a pulsed external field. Influence of modes in altering large scale transport of the classical system has been studied by invoking an equivalent dynamical model, the generalized standard map. The virtue of the generalization arises from the ratio of two length scales, namely, well width and field wave length. This generalization is found to have larger parametric space for existence of AM. For certain parametric values sticky regions (beaches) exist around the accelerator islands. Beaches play a major role in dragging generic chaotic orbits along the modes. This mechanism leads to significant enhancement in momentum transport. Using localized wave packet, effects of accelerator modes in quantum system is studied. In accordance with quantum-classical correspondence principle, dynamics of the wave packet which is placed on the accelerator island reproduces all the classical behaviour. Although beaches are classical structures, they are found to be responsible for enhancing quantum transport. We hope the present study would initiate work to explore accelerator modes as a tool for ionization process in finite quantum well system.

#### Acknowledgement

One of us, VBS, would like to acknowledge the hospitality of the Institute of Theoretical Atomic and Molecular Physics, Harvard University, Cambridge, USA, during August 2002 when this paper was being completed and written.

## REFERENCES

- [1] A.J. Lichtenberg and M.A. Lieberman, *Regular and Chaotic Dynamics*, Springer-Verlag, New York, 1992.
- [2] B.V. Chirikov, Phys. Rep. **52**, 263 (1979).
- [3] M.F. Shlesinger, G.M. Zaslavsky and U. Frish (Eds.), *Lévy Flights and Related Topics in Physics*, Springer-Verlag, 1995.
- [4] R. Ishizaki, T. Horita, T. Kobayashi and H. Mori, Prog. Theor. Phys. **85** (5), 1013 (1991); Y.H. Ichikawa, T. Kamimura and T. Hatori, Physica **29 D**, 247 (1987).
- [5] J.D. Hanson, E. Ott and T.M. Antonsen Jr., Phys. Rev. A **29**, 819 (1984).
- [6] A. Iomin, S. Fishman and G.M. Zaslavsky, Phys. Rev. E **65**, 036215 (2002).
- [7] B.G. Klappauf, W.H. Oskay, D.A. Steck and M.G. Raizen, Phys. Rev. Lett. **81**, 4044 (1999).
- [8] R.M. Godun, M.B. d'Arcy, M.K. Oberthaler, G.S. Summy and K. Burnett, Phys. Rev. A **62**, 013411 (2000).
- [9] S. Fishman, I. Guarneri and L. Rebuzzini, Phys. Rev. Lett. **89**, 084101 (2002); More details are given in nlin.CD/0202047.
- [10] P.B. Wilkinson, T.M. Fromhold, L. Eaves, F.W. Sheard, N. Miura and T. Takamasu, Nature **380**, 608 (1996).
- [11] R. Sankaranarayanan, A. Lakshminarayan and V.B. Sheorey, Phys. Lett. A **279**, 313 (2001).
- [12] S.D. Frischat and E. Doron, Phys. Rev. E, **57**, 1421 (1998).
- [13] M.F. Shlesinger, G.M. Zaslavsky and J. Klafter, Nature **363**, 31 (1993).
- [14] R. Sankaranarayanan, A. Lakshminarayan and V.B. Sheorey, Phys. Rev. E **64**, 046210 (2001).
- [15] G. Casati, B.V. Chirikov, J. Ford and F.M. Izrailev, *Lecture Notes in Physics* Vol.93, 334 (1979)
- [16] F.M. Izrailev and D.L. Shepelyanskii, Theor. Math. Phys. **43**, 553 (1980).
- [17] M. Abramowitz and I.A. Stegun (Ed.), *Handbook of Mathematical Functions*, p. 303, Dover, New York, 1965.
- [18] W. Gautschi, SIAM J. Numer. Anal. **7**(1), 187 (1970).

## FIGURES

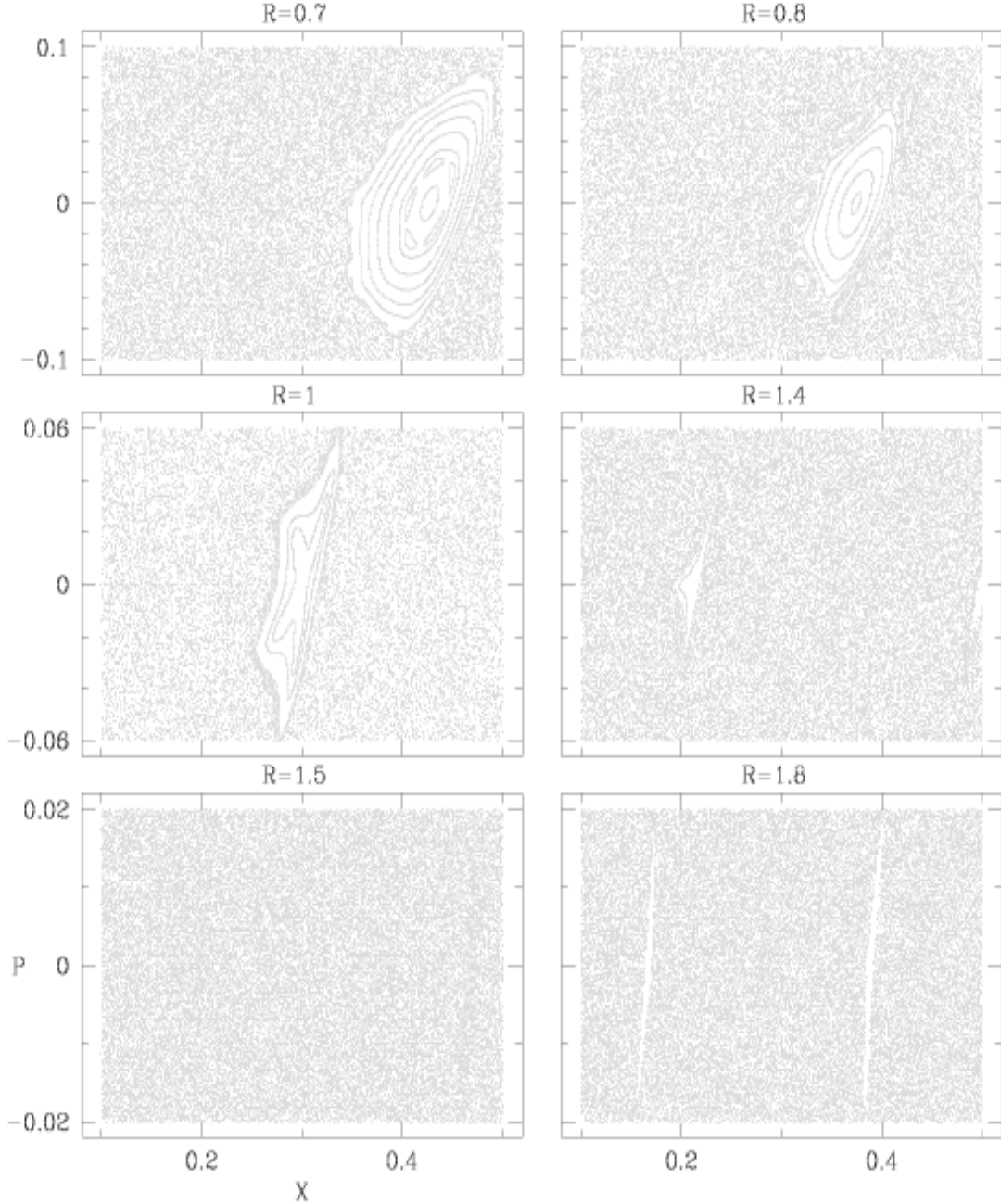


FIG. 1. Stable regions embedded in chaotic sea are the accelerator modes of the well map ( $K/2\pi = 1.05$ ) whose  $P' = 0$  and  $X'$  is positive. For  $R = 0.7, 0.8$  and  $1$ , we observe  $(1, 0)_-$  type mode. For  $R = 1.4$ , one more mode just appears in the phase space which is  $(1, 0)_+$  type. For further increase of  $R$ , both the types are fully visible. Since  $X' \propto 1/R$ , as  $R$  increases the accelerator islands move towards interior of the square well. Note the three different scales on  $P$ -axis.

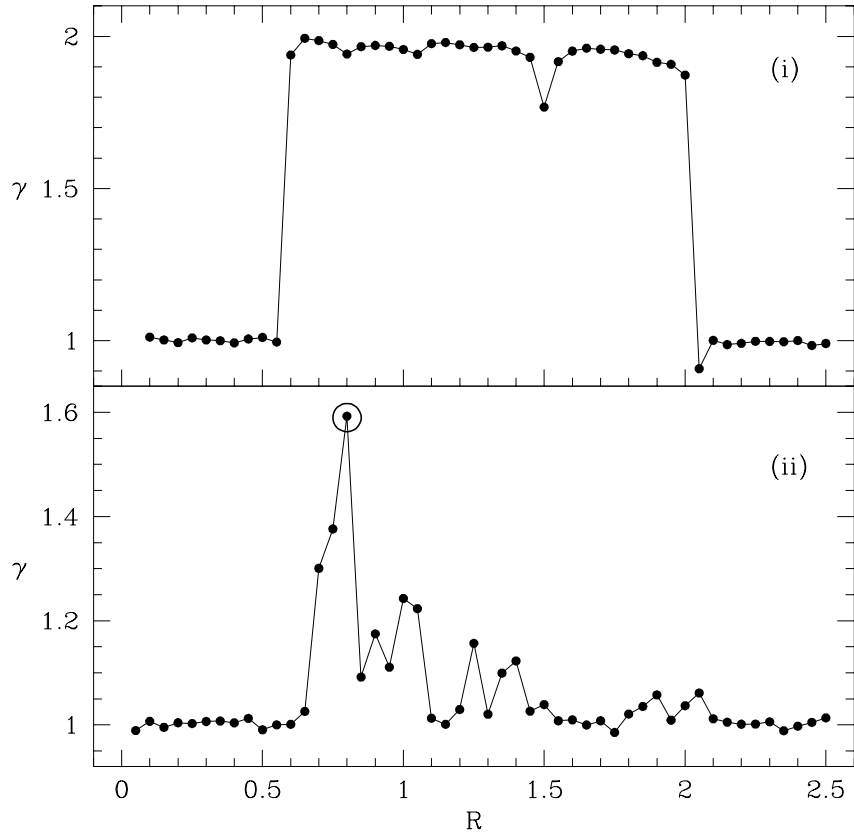


FIG. 2. Exponent  $\gamma$  is plotted with respect to the parameter  $R$  for  $K/2\pi = 1.05$ . To obtain the exponent, an initial ensemble of 10000 phase space points is iterated by the well map for 5000 time steps. For (i) the ensemble consists of points with  $P_0 = 0$  and  $X_0$  distributed uniformly between  $-1/2$  and  $1/2$ . The range of  $R$  given by the Eqn. (11) with  $R_0 = 0.598$  and  $R_1 = 1.988$  is seen as  $\gamma \simeq 2$  due to ballistic evolution of the accelerating points contained in the ensemble. For (ii) the ensemble is chosen from chaotic region of the phase space. Maximum exponent observed for  $R = 0.8$ , marked by circle, is due to the beaches around the AM island.

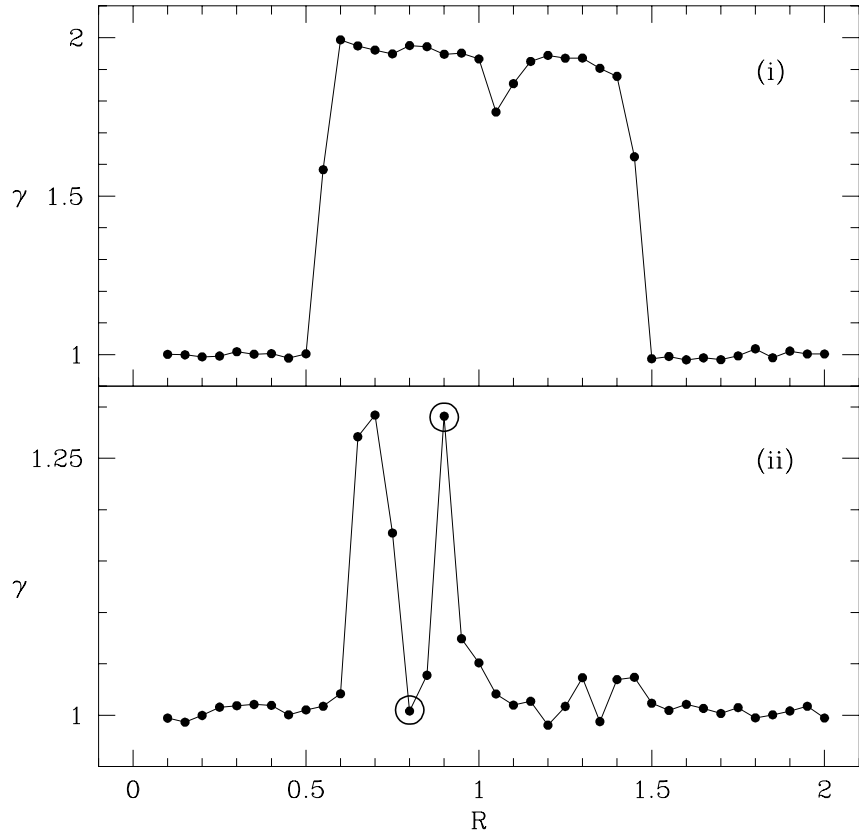


FIG. 3. Exponent  $\gamma$  is plotted with respect to the parameter  $R$  for  $K/2\pi = 2.05$ . Rest of the calculation details are similar to the Fig. 2. In (i) the range of  $R$  given by the Eqn. (11) with  $R_0 = 0.57$  and  $R_1 = 1.41$  is seen as  $\gamma \simeq 2$ . In (ii) the exponents for  $R = 0.8$  and  $0.9$  are marked by circles. Corresponding AM islands for these two cases are shown in Fig. 4.

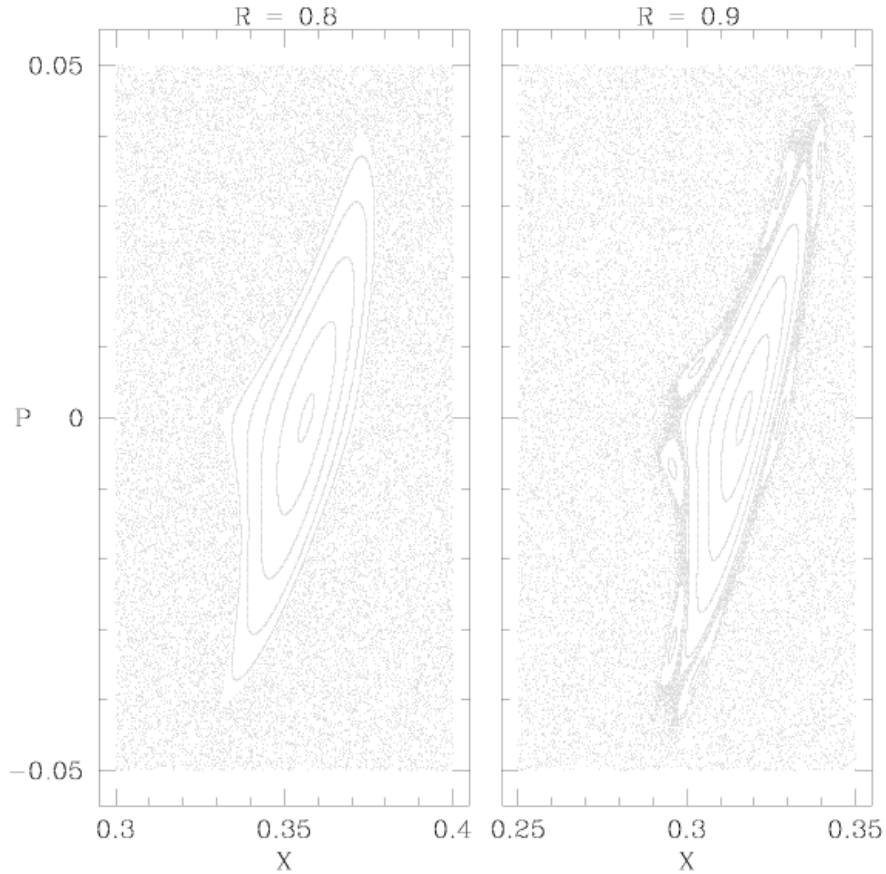


FIG. 4. Step-2 AM are shown for  $K/2\pi = 2.05$ . For  $R = 0.9$ , the AM island is accompanied by a chain of 2/7 resonance zones and sticky beaches. On the other hand, AM island for  $R = 0.8$  is not accompanied by any beach regions.

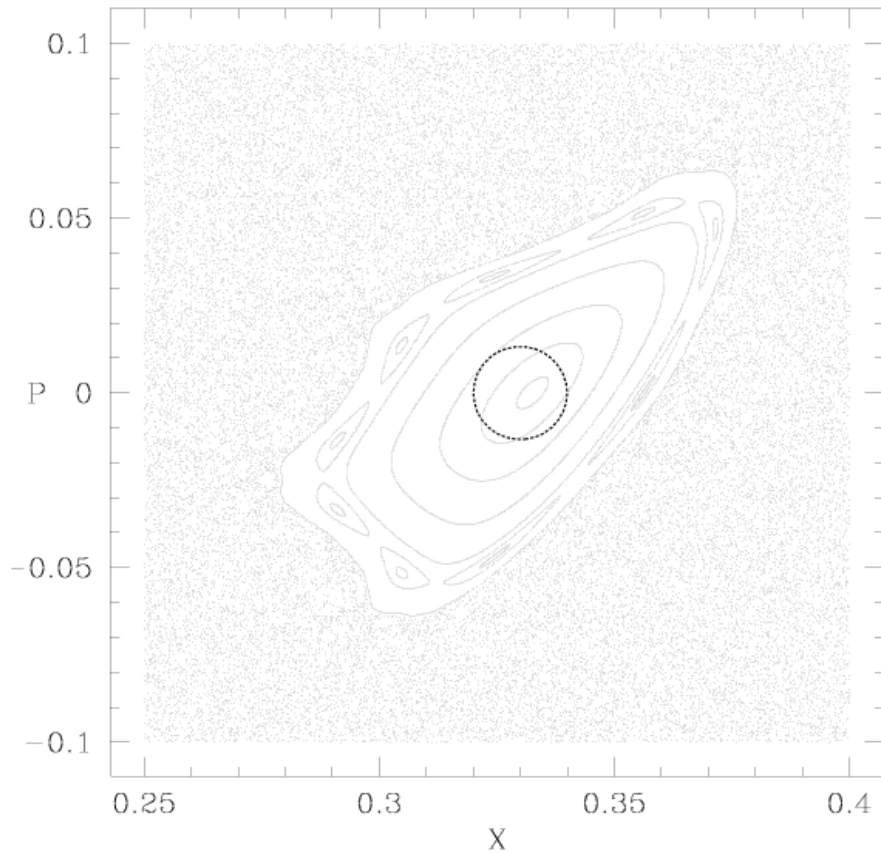


FIG. 5. Stable accelerator island is embedded in chaotic sea for  $K/2\pi = 1.05$  and  $R = 0.9$ . Dashed circle shows location of the initial wave packet in phase space for  $h' = 0.001$ .

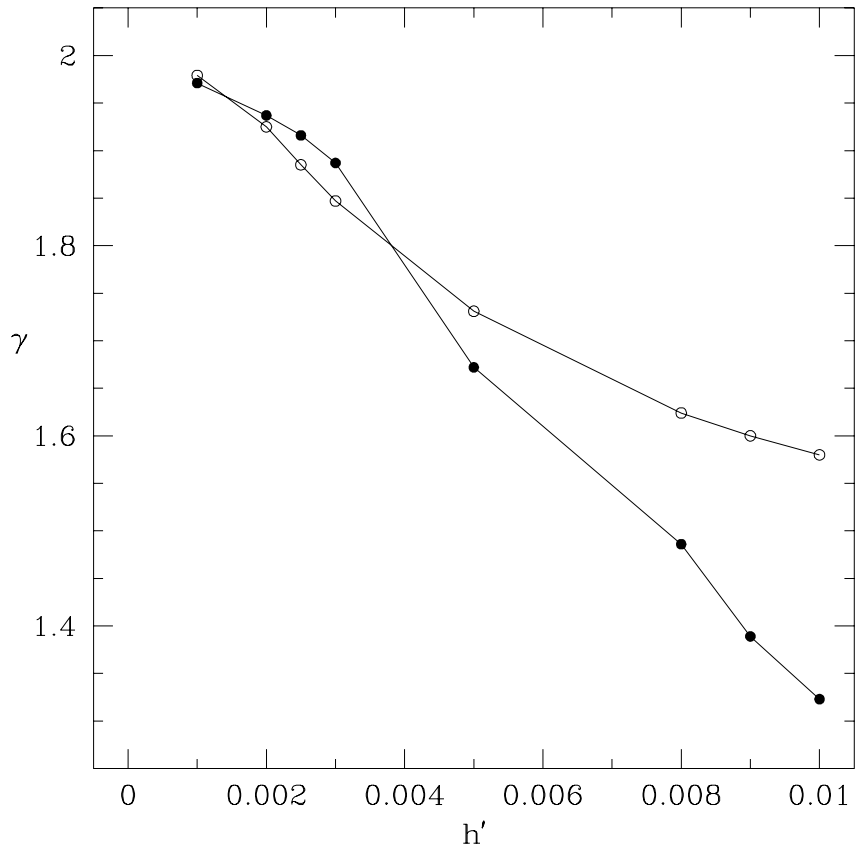


FIG. 6. Filled circle is exponent  $\gamma$  of the quantum energy evaluated up to  $t = 18$ . Open circle is the classical exponent obtained from classical evolution (up to 18 iterations) of corresponding Gaussian ensemble containing 10000 points.

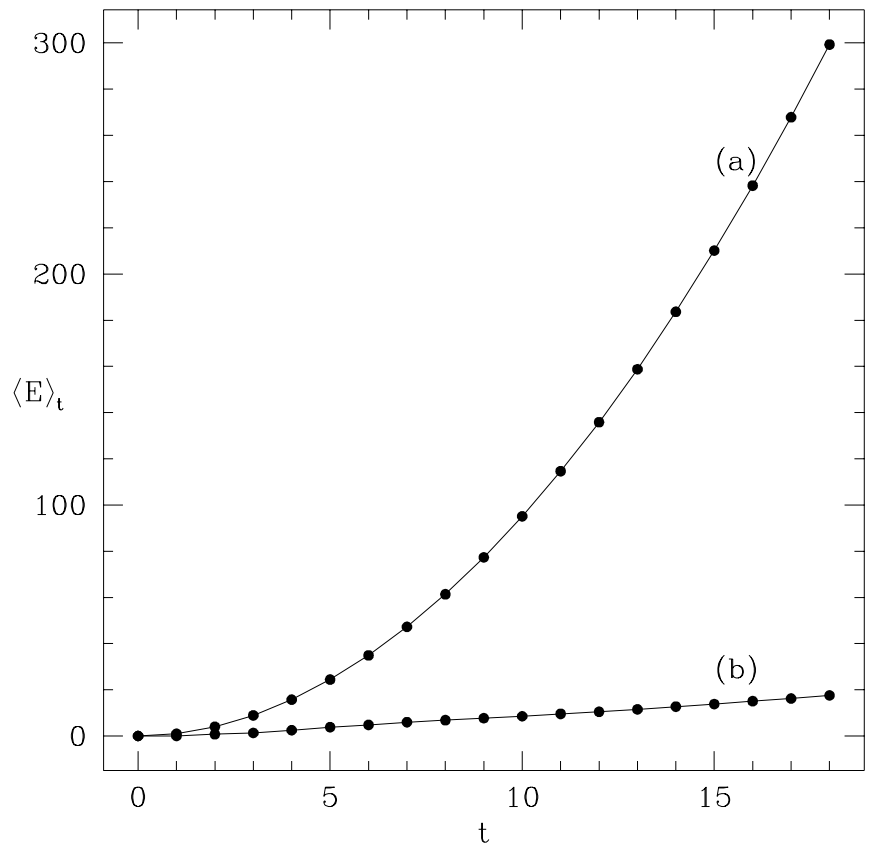


FIG. 7. Quantum energy for the cases (a) and (b) with  $h' = 0.001$ .

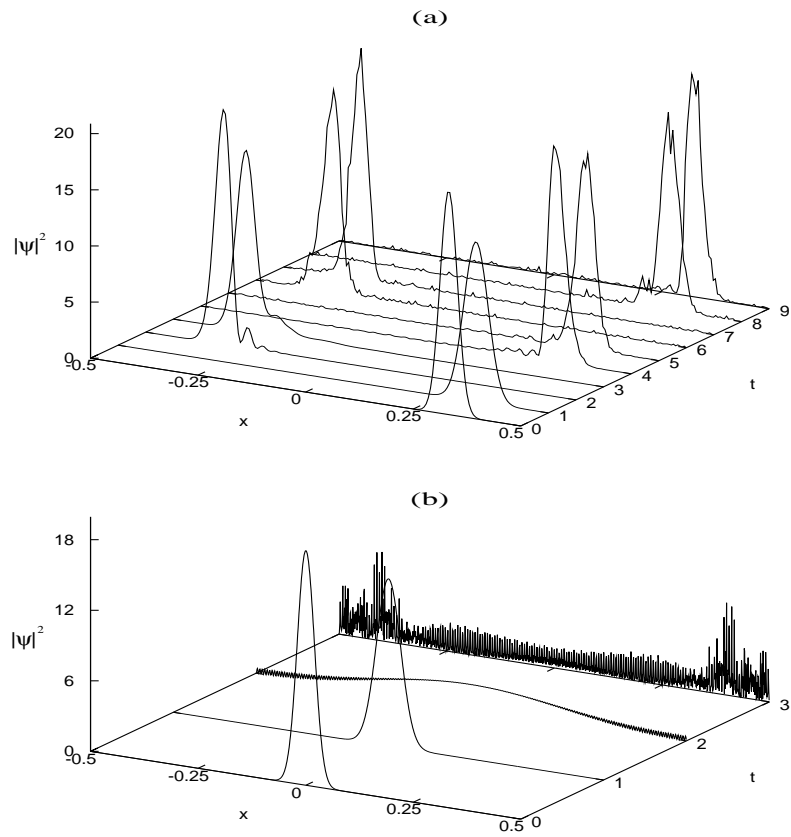


FIG. 8. Evolution of the wave packet for the cases (a) and (b) with  $h' = 0.001$ .

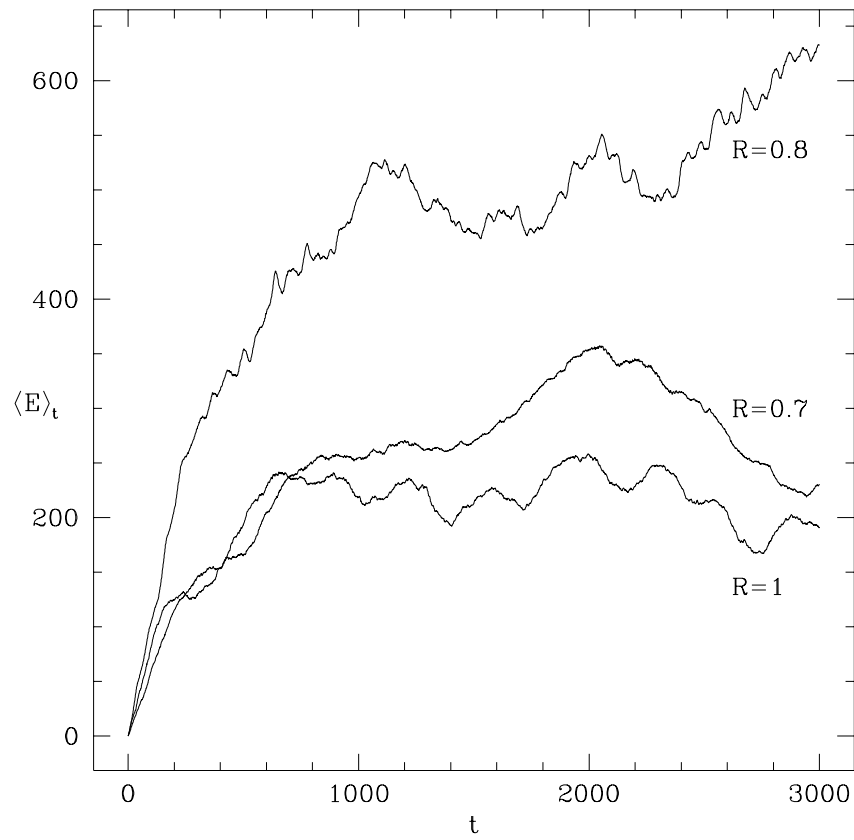


FIG. 9. Kinetic energy of the quantum particle for  $h' = 0.01$ . For  $R = 0.7, 0.8$  and  $1$  the effective field strengths are  $k = 30.3, 26.5$  and  $21.2$  respectively.